

# Electron Density Distributions and Atomic Charges\*

B. Hess

Theoretische Chemie, Universität Bonn, D-W-5300 Bonn, Germany

H. L. Lin, J. E. Niu, and W. H. E. Schwarz

Theoretische Chemie, Universität Siegen, D-W-5900 Siegen

Z. Naturforsch. **48a**, 180–192 (1993); received January 11, 1992

Accurate electron densities and X-ray form factors of Li, Be, F and their ions have been calculated. Electron correlation, crystal fields and ionic charge transfer change the form factors by up to a few percent, mainly in the range of  $\sin \theta/\lambda < \frac{1}{5} \text{ \AA}^{-1}$ . Although electron correlation and crystal fields are small perturbations, their effects on the density and form factor are not additive. Densities or form factors of atomic and ionic systems are very similar;  $[\text{Li}^0\text{F}^0]$  and  $[\text{Li}^+\text{F}^-]$  procystals differ by an effective charge transfer of not more than 0.4 e. Charge transfer and charge overlap in crystals cannot be distinguished uniquely. When the experimental data on  $\text{Li}_2\text{BeF}_4$  (approximately reproduced by 3/4 atomic plus 1/4 ionic procystal) are interpreted from the *atomic viewpoint*, the atomic partial charges are as low as 0.1 e ( $\text{Li}_2^{+0.1}\text{Be}^{+0.2}\text{F}_4^{-0.1}$ ); when interpreted from the *ionic viewpoint*, the charges are much higher, namely 0.7 e. Intermediate viewpoints are also possible.

**Key words:** Electron densities; Form factors; X-ray diffraction; Ionic charges; Ionic bonding.

## 1. Introduction

A basic paradigm of chemistry since Dalton [1] is that matter, i.e. molecules, crystals etc. consists of atoms, which retain a large part of their individuality, and which become only slightly deformed by the chemical interactions. In all present textbooks of general chemistry and solid-state physics, the interatomic interactions are classified as covalent, ionic, metallic, or weak, with transitions between these pure cases. In this context, *partial charges on atoms in compounds* form a useful concept (see e.g. [2]). A serious problem, however, is that there does not exist a universal rigorous definition of atoms and ions in molecules and crystals.

Generally speaking, two different strategies may be chosen to define atomic charges. Historically the first strategy was to define a *simple model* containing charge parameters, and to calculate the experimentally measurable properties with this recipe. Bond energies, cohesive energies, elastic constants, reactivities (branching ratios, rate constants etc.) or spectro-

scopic constants of all kinds of spectra (IR, VIS-UV, Raman, XPS, NMR, X-ray diffraction and scattering etc.) may be used for this purpose. Such an approach is *useful*, if a large body of empirical data can be rationalized with the help of one consistent charge scale.

Alternatively one may start from the wave function, the electron density operator or the electron density distribution. The prescription to extract atomic charges should be constructed in a nonarbitrary manner in order to yield well-defined results. The theoretically most sophisticated approach of this kind has been proposed by Bader [3]. Again, in order to be especially *useful* to chemists and solid-state physicists, the derived charges should fit into the empirical charge scales mentioned above. Theoretically less well founded prescriptions may be more successful in this respect, as for instance Mulliken's population analysis of wavefunctions, especially if based on natural or modified atomic orbitals [4], or Hirshfeld's density partitioning [5].

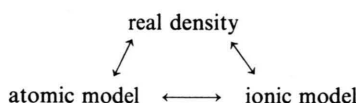
Instead of these *partitioning approaches*, where the total charge distribution is in some sense arbitrarily split up into overlapping [4, 5] or nonoverlapping parts [3, 6], one may also apply *comparative approaches*. A frequent approach, for instance, in X-ray crystallography is to construct so-called promolecules or procystals (chemical formulae in square brackets [ ]) as a

\* Presented at the Sagamore X Conference on Charge, Spin and Momentum Densities, Konstanz, Fed. Rep. of Germany, September 1–7, 1991.

Reprint requests to Prof. Dr. W. H. E. Schwarz, Theoretische Chemie, Universität Siegen, Postfach 10 12 40, D-W-5900 Siegen, Fed. Rep. of Germany.



Diagram 1



superposition of densities of the *independent atoms or ions* ( $\varrho_{\text{iam}}$ , iam = independent atom model) and to compare and to adjust these promolecules to the density of the real compound ( $\varrho$ ), in reciprocal or in position space (see diagram 1). Routinely, the positions of the atoms in a crystal are determined by minimizing the density difference

$$\Delta\varrho = \varrho - \varrho_{\text{iam}} \quad (1)$$

in the weighted-least-squares sense (actually  $\Delta F(\varrho, \varrho_{\text{iam}})$  is minimized in reciprocal space). It has been suggested by Dunitz and Seiler [7] to determine also the atomic charges  $p$  from

$$p \text{ so that } \frac{d}{dp} \int d\tau (\Delta\varrho(p))^2 = 0 \quad (2)$$

with

$$\Delta\varrho(p) = \varrho - p \cdot \varrho_{\text{iam}}^{\text{ions}} - (1 - p) \cdot \varrho_{\text{iam}}^{\text{atoms}}. \quad (2a)$$

A similar approach has also been suggested by Schwarz et al. [8], both in position and reciprocal space.

Reservations against the very concept of atomic charges may be found in the literature, too (e.g. [9]). Dunitz [7], for instance, mentioned “the fact that it is *easier* to calculate many properties of (molecules and) solids with (point) charges than with charge distributions, making the ionic (point charge) model more convenient, but it does not necessarily make it more *correct*”. Obviously, ions and partial charges on atoms in matter are not originally given by nature (for the opposite standpoint see Bader [3]), but they form a useful concept to *understand* the nature of matter. The concept of ions is to be judged not under the categories “correct or wrong”, but “more or less useful”. The relevant questions concern reliable recipes to extract chemically useful charge scales for observable data.

Anyhow, it seems natural and attractive to derive charges on atoms in compounds directly from the charge distribution in the compound. Such charges, which are reproducible, though model-dependent properties obtained from observables, are still “non-observables” in the strict quantum-mechanical sense. The question to be addressed in this paper is, what kind of atomic charges can be obtained by the comparative approach from a given distribution  $\varrho$ . We remember that both  $\varrho$  and  $\varrho_{\text{iam}}$  are orders of magnitude greater than  $\Delta\varrho$  in most parts of space. Further

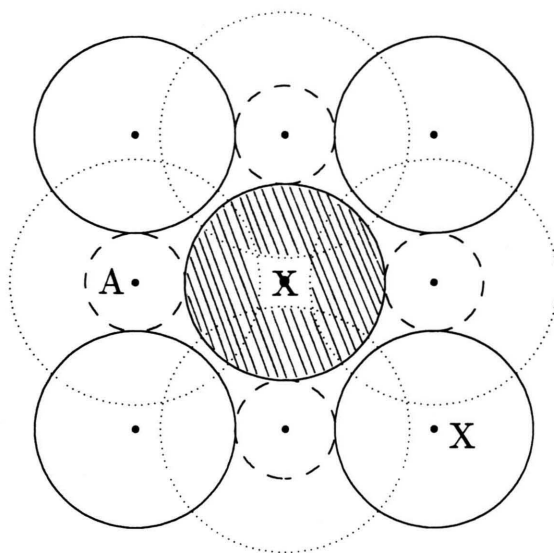


Fig. 1. Sketch of the density distribution in an “ionic crystal”  $A^+X^-$ . Bold circles represent halogen ions  $X^-$  with an excess electron, dashed circles represent alkali ions  $A^+$ . The corresponding “atomic crystal”  $A^0X^0$  has no excess electron on  $X$  (spatial extension comparable to  $X^-$ , bold circles), but the diffuse valence electron density of the surrounding  $A^0$  (dotted circles) contributes additional density to the valence shell of  $X$  (hatched area).

more, as mentioned already by James [9] or Slater [10] many years ago, the densities of superimposed atoms and of superimposed ions are quite similar (see Figure 1). Therefore, highly accurate data are needed both for the crystal density  $\varrho$ , and for the atomic and ionic reference densities  $\varrho_{\text{iam}}^{\text{(neutral)}}$  and  $\varrho_{\text{iam}}^{\text{(ionic)}}$ .

In the next section, we comment at first on the choice of accurate atomic and ionic reference densities. In the third section, we discuss appropriate stabilizing potentials for negative atomic ions. In the fourth section, we report on the calculation of correlated many-particle wave functions for atoms and ions with and without a model potential. In the fifth section the calculated densities in real space and form factors in reciprocal space are analysed. In Sect. 6 we discuss the resulting densities of atomic and ionic procystals of  $\text{LiF}$  and report on the application of the corresponding form factors to the determination of charge distributions in  $\text{Li}_2\text{BeF}_4$  crystals. Section 7 contains the summary and our conclusions that ionic crystals resemble a superposition of ions as well as a superposition of atoms, and that physically and chemically useful ionic charges therefore cannot be obtained in a straightforward way from the charge distribution of ionic crystals by the comparative approach.

## 2. Atomic and Ionic Reference Densities

Concerning *atomic reference* densities, the standard crystallographic choice is that of an ensemble density of free atoms *in vacuum*, spherically averaged over all low-lying states of the ground configuration [11] (note that most crystallographers do *not* choose the atomic ground state as their reference state *but* the ground configuration states average). The (relativistic) Hartree-Fock approach is a reasonable approximation for the density of the atomic cores; accordingly (symmetry-restricted) average-state Hartree-Fock form factors [11] are used in nearly all crystallographic structure and charge-density works. The fractional change of the densities owing to many-particle correlations, however, may be significant, especially for the valence shells, so that the Hartree-Fock approximation is not completely satisfactory. Accordingly, correlated atomic densities and form factors should be used if high accuracy is demanded. The treatment of electron correlation will be described in Section 4.

Concerning *ionic reference* densities, there are additional problems. Whereas all positive and many singly charged negative ions are stable in vacuum, no multiply charged atomic anions (as, for instance,  $O^{-2}$  or  $S^{-2}$ ) exist in field-free space. Singly charged anions have rather diffuse charge distributions and are subject to pronounced electron correlation effects, which stabilize them considerably with respect to the Hartree-Fock approximation. Free “doubly charged anions” are not bound at all, the second excess electron being at infinity. Neglect of electron correlation at the unrestricted Hartree-Fock level makes them even more unstable against immediate autoionization. In quantum-mechanical calculations it is common to impose the spatial-symmetry restriction on the orbitals, which further destabilizes the anion energetically but artificially prevents autoionization. It is difficult to see what the physical meaning of restricted Hartree-Fock calculations of atomic anions in vacuum might be. Nevertheless, the corresponding form factors are tabulated in the literature [11] and are commonly used without hesitation.

In real systems, negative ions become stabilized by the polar environment, which creates a potential well at the site of the anion (potential stabilization) and a pseudopotential barrier around the anion because of the Pauli exclusion effect with respect to the occupied shells of the surrounding cations and anions (overlap compression). Physically it is much more reasonable

to stabilize the negative atomic reference ions by some *realistic model potential* than by the artificial symmetry restriction of the Hartree-Fock approximation. It is widely accepted to choose the neutral atom's *reference density* (for use in an “atomic” procrystal) from an atomic calculation in a *spherically symmetric potential* (nuclear Coulomb attraction and surrounding vacuum). According to crystallographic tradition the same convention of spherical symmetry will also be chosen for the ionic reference [11]. Of course, atoms and ions *are* deformed by covalent and also by ionic interactions; for instance, p-AOs are indispensable for any reasonably accurate description of bonded hydrogen atoms, and d- and even f-AOs in the cases of second and third-row atoms (C, Si etc.) Just these chemically important polarizations or deformations of atoms and ions by the surrounding matter can then be seen in the  $\Delta\rho$  map of the density difference with respect to the spherical atoms and ions.

## 3. Potential for the Atomic Ions

We suggest to determine the potential for the atomic ions as the spherical average of the electrostatic potential in a corresponding crystal lattice of point charges (Madelung potential  $V_M$ ). Our theoretical data will later be applied to the analysis of highly accurate X-ray diffraction data of  $Li_2BeF_4$  [7, 29]. This compound had been chosen for the following two reasons: a) the relative density changes between atoms and ions are most pronounced for light systems such as Li, Be, O, or F; b) ionic density changes in the outer valence shells of atoms can, by X-ray diffraction, best be detected at low scattering angles, which will appear for crystals with large unit cells such as  $Li_2BeF_4$  (space group  $R\bar{3}$  with 126 atoms in the hexagonal unit cell of  $V = 1365 \text{ \AA}^3$ ).

The coordinates of  $Li_2BeF_4$  were taken from the crystal structure in [12], and integer charge values of  $Li^{+1}$ ,  $Be^{+2}$ , and  $F^{-1}$  were chosen. The two weakly nonequivalent  $Li^{+}$  ions and the  $Be^{+2}$  ion are approximately tetrahedrally surrounded by four weakly nonequivalent  $F^{-}$  ions at distances in the range of  $R_{LiF} = 3.53 \pm 0.05 a_0$  ( $\approx 1.87 \text{ \AA}$ ) and  $R_{BeF} = 2.94 \pm 0.01 a_0$  ( $\approx 1.56 \text{ \AA}$ ), respectively, whereas the  $F^{-}$  ions are roughly trigonally surrounded by two  $Li^{+}$  and one  $Be^{+2}$  with the  $F^{-} \sim 0.25 a_0$  above the  $Li_2Be$ -plane.

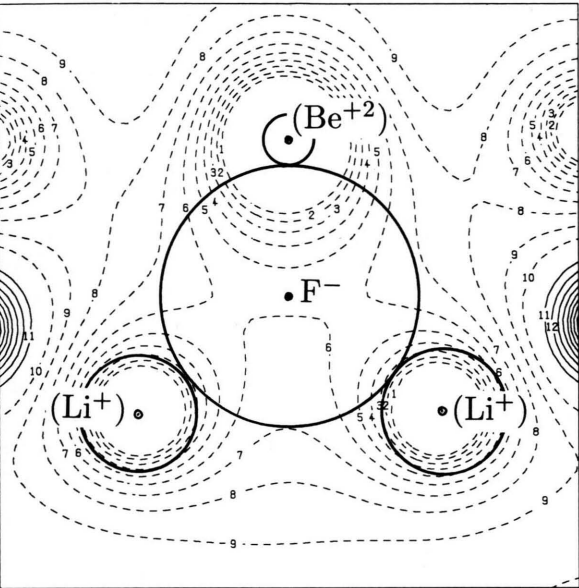


Fig. 2. Madelung potential  $V_M$  in  $\text{Li}_2^+\text{Be}^{+2}\text{F}_4^-$  around  $\text{F}^-$  (cryst. position I) on a plane of  $5.67 \text{ \AA} \times 5.67 \text{ \AA}$  through  $\text{F}^-$  parallel to the plane through the adjacent two  $\text{Li}^+$  and one  $\text{Be}^{+2}$ , lying  $\approx \frac{1}{4} a_0$  lower. Distance of contour lines is  $0.1 \text{ a.u.} \approx 2.72 \text{ Volt}$ . --- positive potential (attractive for negative electrons); — negative potential; the zero-potential line is not shown. The bold circles indicate the standard ionic spheres with the ionic radii given in Table 1.

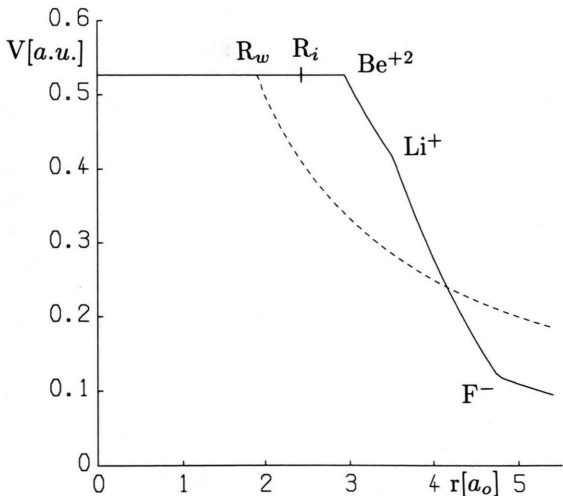


Fig. 3. Spherical component  $V(r)$  of the Madelung potential  $V_M$  (attractive for negative electrons) in  $\text{Li}_2^+\text{Be}^{+2}\text{F}_4^-$  around  $\text{F}^-$  (I). The dashed line represents the Watson potential  $V_w$ .  $R_w$  = Watson radius of  $\text{F}^-$ ,  $R_i$  = ion radius of  $\text{F}^-$ . The positions of the nearest-neighbour ions  $\text{Be}^{+2}$ ,  $\text{Li}^+$  (2 ones) and  $\text{F}^-$  (4 ones) are also indicated.

With the help of a program from Roos and Wahlgren [13], the Madelung potentials around the different ions were calculated according to the method of Ewald and Bertaut [14]. In Fig. 2 a contour plot of the Madelung potential around  $\text{F}^-$  at crystallographic position (I) is presented.

Within the “volume” of  $\text{F}^-$  there is a significant variation of the electrostatic crystal potential, especially in the neighbourhood of the  $\text{Be}^{+2}$  cation: the crystal potential is far from being constant inside the anion. (This asymmetry will cause a polarization of the  $\text{F}^-$  ion towards the  $\text{Be}^{+2}$  ion, which will show up in the deformation-density map [7, 29] and is sometimes interpreted as an indication of covalency.) When we determine the spherically symmetric monopole component  $V(r)$  around the F nucleus (Fig. 3), we obtain a constant potential inside  $\text{F}^-$  up to  $R = 2.945 a_0$ , which is the nearest-neighbour ( $\text{Be}^{+2}$ ) distance. The potential then drops sharply as  $V = \text{const} + 2/r$ . Further decrease of the potential starts at the two F–Li distances around  $3.5 a_0$ .

The effective potential felt by the fluorine electrons is smaller than this electrostatic potential in the region of the outer tails of the surrounding ions because of Pauli’s exclusion principle. Therefore we choose the simple Watson potential  $V_w(r)$  [15] as an appropriate model potential (as done already earlier, for instance, by Weiss et al. [26]),

$$V_w(r) = \begin{cases} -Z_i/R_w & \text{for } r \leq R_w, \\ -Z_i/r & \text{for } r \geq R_w, \end{cases} \quad (3)$$

which is smaller than the electrostatic potential for  $r > R_w$  (see the dashed curve in Figure 3).  $Z_i$  is the charge of the central ion, and  $R_w$  is the so-called Watson radius, which is defined here by matching the spherically averaged Madelung potential  $V$  with  $V_w$  in the core region. The corresponding Watson radii are given in Table 1. We note that there is no simple relation between the ionic radii and the Watson radii;

Table 1.

Inequiv. ions (coordination no. in parenth.)	Standard ion radius in $a_0$	Watson sphere: radii* in $a_0$ (its charge in $ e $ )	Madelung potentials* in eV
2 $\text{Li}^+$ , (4)	1.11	2.12–2.14, (–1)	$12.76 \pm 0.06$
$\text{Be}^{+2}$ , (4)	0.51	2.17, (–2)	25.13
4 $\text{F}^-$ , (3)	2.45	1.88–1.91, (+1)	$14.31 \pm 0.1$

\* Slightly different potentials and radii for the nonequivalent crystallographic positions.



the ionic radii depend on the respective ions themselves, whereas the Watson radii are determined by the Madelung potential of the surrounding charge lattice.

#### 4. Correlated Wavefunctions of Atoms and Ions in Spherical Potentials

The atomic-density and form-factor calculations were performed by the *basis-set expansion* method using Cartesian Gaussians. According to the literature [16], up to f-functions are needed to obtain accurate correlated densities. For *beryllium* we used the [8s 5p 2d 1f] basis given in [17] and augmented it by a p- ( $\zeta=12.5$ ) and a d-function ( $\zeta=2.0$ ), yielding an [8s 6p 3d 1f] basis. The *fluorine* basis was taken from [18], but contracted as [4221...] and augmented by a diffuse d-function ( $\zeta=0.1$ ) yielding an [8s 8p 5d 2f] basis. For *lithium*, where the L-shell correlation is weak, the basis of [19] was reduced by the most diffuse d-function ( $\zeta=0.045$ ) and all f-functions, leaving an [11s 11p 7d] basis in the contraction scheme [311...]. Six-component d-functions and ten-component f-functions were used throughout. The decision to add or delete specific functions was based on the magnitude or smallness of the numerical changes observed in the correlated atomic form factors finally obtained.

The atomic wavefunctions of Li, Be, F and their ions were calculated by means of ab-initio SCF and CI methods, using the MRD-CI (multi-reference double-excitation configuration-mixing) program package of Buenker and Peyerimhoff [20]. Since the programs can only handle the largest *Abelian* subgroup of the full-symmetry group, special care had to be exercised to ensure that the resulting one-particle basis for the configuration-mixing treatment is adapted to spherical symmetry. All calculations started from a Hartree-Fock (SCF) calculation for the corresponding closed-shell system ( $F^-$ , Be,  $Be^{++}$ ,  $Li^+$ ).

The SCF orbitals thus obtained were used to generate symmetry-adapted natural orbitals (NOs) from the density matrix of a singles-doubles CI for the atom or ion under consideration. According to [16, 21], triple and quadruple excitations do not seem negligible especially in the cases of Be and  $F^-$ . Therefore MR-CI calculations have been performed for these two species, whereas only a single main configuration was used as the reference in the SD-CI calculations of  $Li^+$ , Li,  $Be^{++}$  and F. Configurations with weight (squared coefficient)  $> 0.005$  were included in the refer-

ence set. In the cases of Be and  $F^-$ , the configuration-reference spaces consisted of  $1s^2 2s^2$ ,  $1s^2 2p^2$ ,  $1s^2 2p 3p$  and of  $1s^2 2s^2 2p^6$ ,  $1s^2 2s^2 2p^4 3p^2$ , respectively. For both fluorine systems,  $F^0$  and  $F^-$ , the CI could not be carried out in full because of limitations of the program, and an energy selection threshold of  $10^{-7}$  a.u. was employed in a configuration selection procedure. The NOs obtained were used, in turn, as the one-particle basis for an improved MR-SD-CI. This iterative NO step was repeated once, and from the final one-particle density matrix the radial densities and form factors were calculated.

The SCF energies are near the Hartree-Fock limit (within the order of meV for the Li and Be systems, and within 0.1 eV for F and  $F^-$ ). In the cases of F and  $F^-$ , 90% of the correlation energies were recovered [21], 95% for Be and even more for  $Be^+$ , Li and  $Li^+$ .

#### 5. Form Factors and Radial Densities

##### *Accuracy*

The coherent elastic X-ray scattering form factor  $f$  is the Fourier transform of the one-particle density  $\varrho$ , which is easily obtained from the spherically averaged one-particle density matrix or the corresponding Natural Orbitals and their fractional occupation numbers [22]. The Fourier transforms of the corresponding GTO expansions were determined analytically using the approaches given in [23]. At the SCF level, the finite basis sets resulted in errors of  $f$  of  $\sim 10^{-4}$  e (Li) to  $\sim 10^{-3}$  e (F), i.e.  $\sim 0.01\%$  in the range of  $\sin \theta/\lambda < 1 \text{ \AA}^{-1}$ , as compared to the standard atomic form factors for atoms and ions given in the International Tables [11]. From a comparison with very accurate correlated form factors of the free atoms and ions of Li and Be [16, 22, 24], we estimate our error to be below 0.1%, but up to slightly more than 0.1% for some small values of  $\sin \theta/\lambda < 0.4 \text{ \AA}^{-1}$ . These errors are mainly due to the limitation of the one-particle basis, which contains only a few functions of higher angular momentum. Since correlation corrections to  $f$  are in the percent-range, they are correctly recovered at the semiquantitative level. In an early paper by Tanaka and Sasaki [25], however, where 60 to 90% of the L-shell correlation energy were recovered for different atoms and ions only, significantly less than 50% of the correlation correction to  $f$  in the interesting low  $\sin \theta/\lambda$  range had apparently been obtained. Concerning  $\varrho$ , we may use the very accurate results of Esquivel

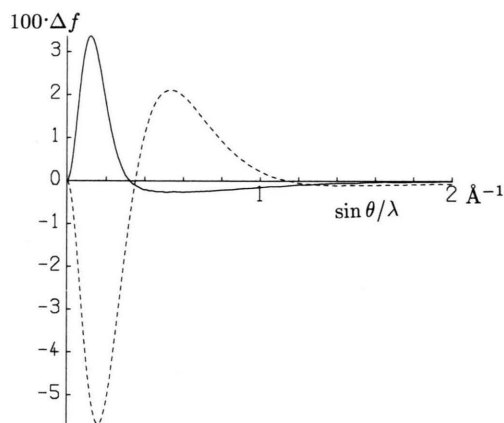


Fig. 4. Change of atomic/ionic form factors owing to electron correlation (CI minus SCF results),  $\Delta^{\text{corr}} f(\text{vac})$ , for Be (—) and for  $\text{F}^-$  (---) in vacuum.

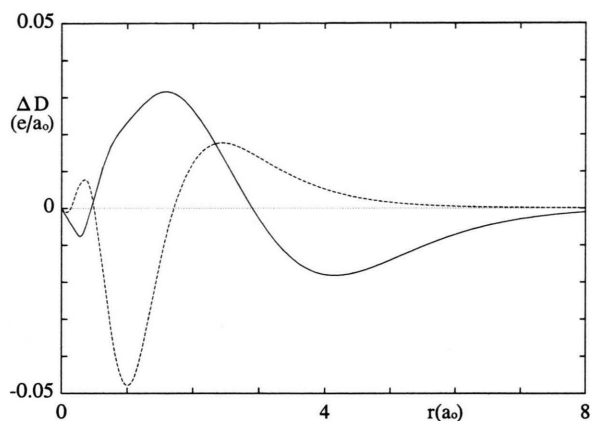


Fig. 5. Change of radial density  $D = 4\pi r^2 \rho$  owing to electron correlation (CI minus SCF results),  $\Delta^{\text{corr}} D(\text{vac})$ , for Be (—) and for  $\text{F}^-$  (---) in vacuum.

et al. [16] on  $\text{Li}^0$ ,  $\text{Be}^0$  and  $\text{Ne}^0$  as reference (note that there is an inconsistency of a factor of  $4\pi$  in the data of [16]). Then the present accuracy for  $\rho$  seems to be similar to that of  $f$ , namely of the order of several 0.01% at the SCF level and about 0.1% for the correlated densities in the  $r$ -range  $< 5 \text{ \AA}$ .

### Correlation Effects

In Fig. 4 we present the influence of correlation on the form factors of free  $\text{Be}^0$  (similar to that of [16, 22]) and free  $\text{F}^-$ . The correlation effects in  $\text{Li}^{+1}$  and  $\text{Be}^{+2}$  with a rather stiff K-shell, and also in  $\text{Li}^0$  are by more than one order of magnitude smaller [16, 24]. The largest  $\Delta^{\text{corr}} f$ -value of Be at  $\sin \theta / \lambda = 0.12 \text{ \AA}^{-1}$  is  $+0.034$  or 1.2%. The  $\Delta^{\text{corr}} f$  curve corresponds to the density decrease in the outer range of the valence shell ( $2-4 a_0$ ) and in the core ( $\sim 0.3 a_0$ ), and to the density increase in the inner region of the valence shell around  $1 a_0$  (see Figure 5). The correlation effects in  $1s^2 2s^2 2p^6 \text{ F}^-$  are quite different from those of  $1s^2 2s^2 \text{ Be}^0$ . The dashed curve in Fig. 4 exhibits two pronounced extrema, a minimum at  $\sin \theta / \lambda = 0.17 \text{ \AA}^{-1}$  ( $\Delta^{\text{corr}} f = -0.056 \sim -0.8\%$ ) and a maximum at  $\sin \theta / \lambda = 0.55 \text{ \AA}^{-1}$  ( $\Delta^{\text{corr}} f = +0.021 \sim +0.8\%$ ). The tendency of the electrons to avoid each other results in a dominant  $s^2-p^2$  angular correlation in Be, combined with a radial compression of the valence density, whereas in  $\text{F}^-$  there is a dominant radial correlation resulting in a flattening of the radial L-shell maximum. Owing to correlation, the density of  $\text{F}^-$  increases in the outer part of the valence shell ( $r > 1.5 a_0$ ) and in the core

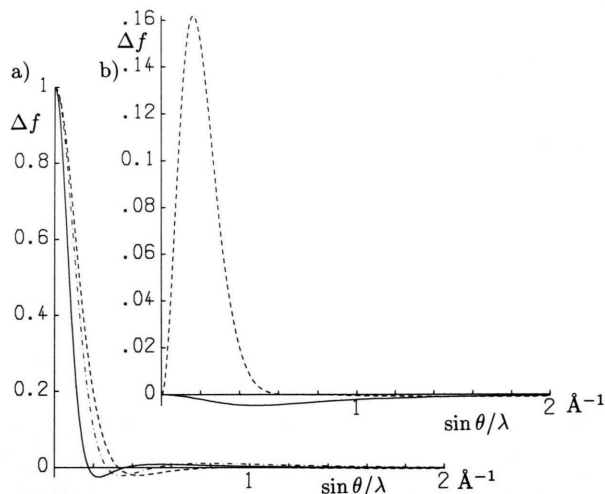


Fig. 6. a) Difference of form factors of atoms and their ions,  $\Delta^{\text{ion}} f(\text{corr, vac})$  (CI results in vacuum).  $\text{Li}^0-\text{Li}^+$ : —;  $\frac{1}{2}(\text{Be}^0-\text{Be}^{+2})$ : ---;  $\text{F}^--\text{F}^0$ : ----. b) Difference of form factors of ions in vacuum and in Watson potential  $\Delta^{\text{pot}} f(\text{corr})$  (CI results). ----:  $\text{F}^-$ ; —:  $\text{Be}^{+2}$  (in an artificially increased Watson potential with  $R_w/2$  instead of  $R_w$ ; otherwise no effect would be visible).

region ( $r < 0.4 a_0$ ) and decreases in the inner valence shell ( $r \sim 0.8 a_0$ ), see Figure 5. The qualitative difference between Be and Ne has also been noted, for instance, by Esquivel and Bunge [16].

### Ionic Effects

In Fig. 6a we present the form-factor difference between the atoms and the free ions at the CI level. They

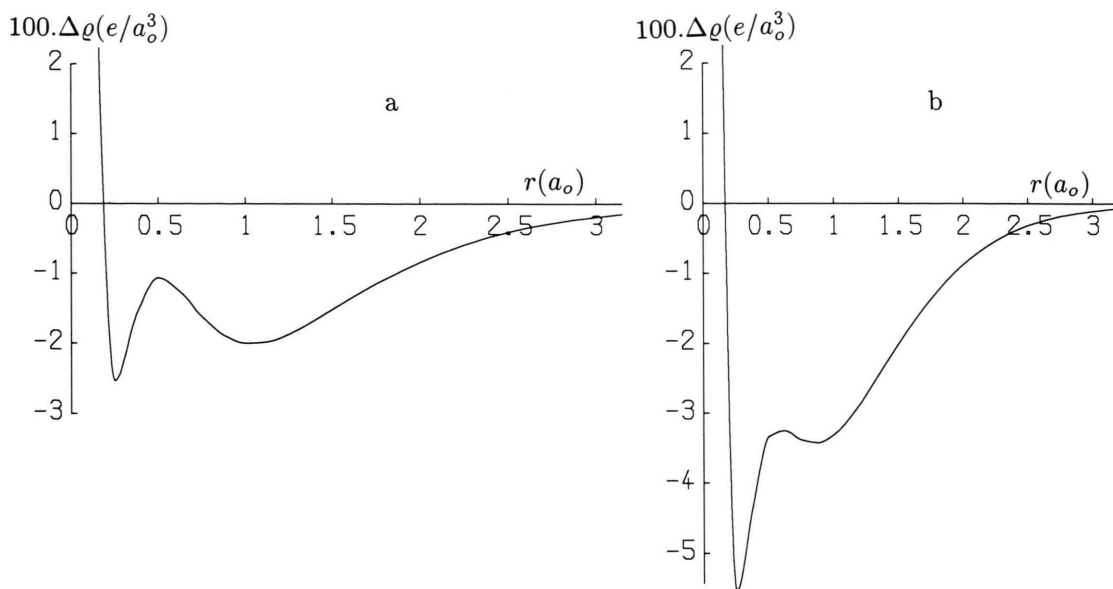


Fig. 7. Change of charge density distribution upon formation of a negative fluorine ion,  $\Delta^{\text{ion}} \rho$ . a)  $F^-$  (in vacuum)  $- F^0$ . b)  $F^-$  (in Watson potential)  $- F^0$ .

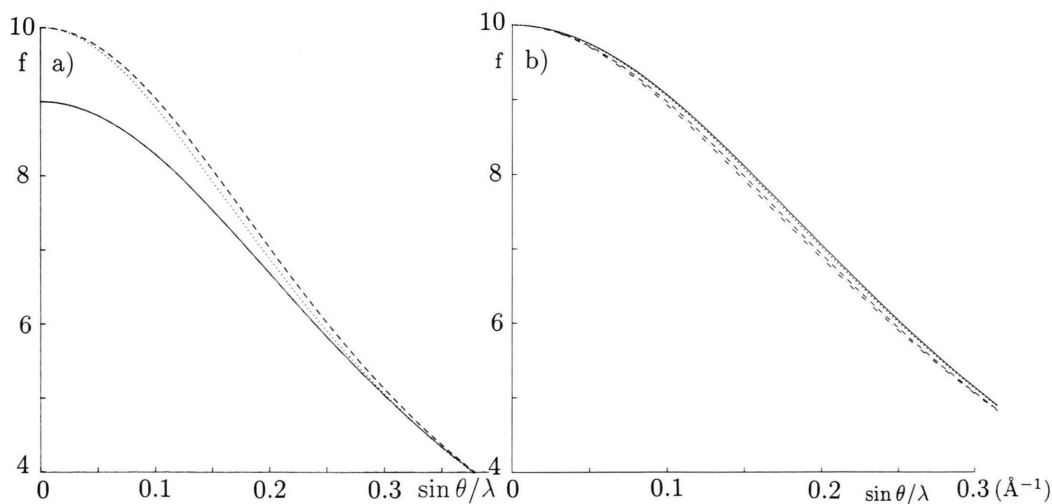


Fig. 8. a) Form factor  $f$  (CI results) of  $F^0$  (—),  $F^-$  in vacuum ( $\cdots$ ) and  $F^-$  in a Watson potential (---). For  $\sin \theta / \lambda > 0.5 \text{ \AA}^{-1}$ , the differences are very small. b) Form factors  $f$  of the  $F^-$  ion: --- SCF, in vacuum; - · - · - correlated, in vacuum; — SCF, in Watson potential;  $\cdots$  correlated, in Watson potential.

do not differ qualitatively from the corresponding Hartree-Fock approximation as given in the International Tables [11]. The ionic effects are also only important for  $\sin \theta / \lambda \leq 0.3 \text{ \AA}^{-1}$ . The density change upon the negative-ion formation of fluorine is shown in Figure 7. The free  $F^-$  has a diffuse, extended density of the excess electron between  $r = 2 a_0$  and  $r \gg R_{\text{ion}} = 1.3 \text{ \AA} = 2.45 a_0$ .

### Crystal-Field Effects

The charge distribution of  $F^-$  is compressed by the external Watson potential. The influence on the form factors had already been investigated at the Hartree-Fock level of approximation by Suzuki and by Weiss et al. [26] and by others (compare, e.g., Schwarz et al. [27]). In Fig. 8a we present our CI results for neutral

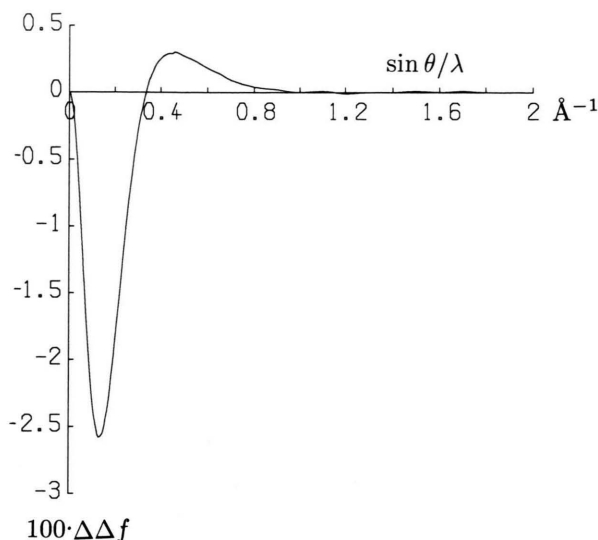


Fig. 9.  $\Delta\Delta f$  for  $F^-$ , see text and diagram 2.

$F^0$ , for the free  $F^-$  ion, and for the  $F^-$  ion in a Watson potential. The modification of the correlated form factor of  $F^-$  by the Watson potential is displayed in Figure 6b. A maximum of  $\Delta^{\text{pot}}f = 0.16 \sim 2.2\%$  is found at  $\sin \theta/\lambda = 0.19 \text{ \AA}^{-1}$ . For the cations, the Watson-potential effects are, of course, of opposite sign, and they are negligibly small (see Figure 6b). The crystal-field effects on  $F^-$  are partially canceled by electron correlation. Therefore the difference between the restricted-Hartree-Fock result and the correlated  $F^-$  in the Watson potential (--- and  $\cdots$  in Fig. 8b) is small. The same may be expected for all halides  $X^{-1}$ , but not for the chalcogenides  $Y^{-2}$  and pnictides  $Z^{-3}$ .

### Cross Effects

In Fig. 8b we compare the form factors of  $F^-$  in vacuum and in a Watson potential, at the SCF and CI levels. The distances between pairs of curves vary in different manners, i.e. the correlation and Watson-potential effects on  $f$  are not additive (contrary to what might have been expected from perturbation theory for small individual effects):

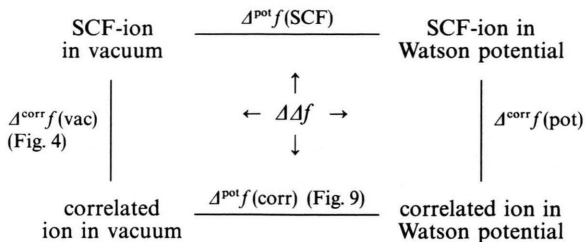
$$\Delta^{\text{corr}}f(\text{vac}) + \Delta^{\text{pot}}f(\text{corr}) = \Delta^{\text{corr}}f(\text{pot}) + \Delta^{\text{pot}}f(\text{SCF}) \quad (4a)$$

but

$$\begin{aligned} \Delta^{\text{corr}}f(\text{pot}) - \Delta^{\text{corr}}f(\text{vac}) \\ = \Delta^{\text{pot}}f(\text{corr}) - \Delta^{\text{pot}}f(\text{SCF}) = \Delta\Delta f \neq 0, \quad (4b) \end{aligned}$$

where the symbols are explained in diagram 2. The nonadditivity ( $\Delta\Delta f$ ) for  $F^-$  is shown in Figure 9.  $\Delta\Delta f$  has a deep minimum at  $\sin \theta/\lambda = 0.13 \text{ \AA}^{-1}$  of about 0.3% ( $-0.026 e$ ), whereas the correlation and Watson-potential effects individually amount to up to  $\sim 1$  and  $\sim 2\%$ , respectively, of the total  $f$  values.

Diagram 2



## 6. Atomic Charges in Ionic Compounds

With reliable and accurate atomic and ionic densities at hand, we will first compare the densities of atomic and ionic procrystals. As representative examples we choose the diamond structure with an interatomic distance of  $1.54 \text{ \AA}$ , and the face-centred cubic LiF structure with an interionic distance of  $2.01 \text{ \AA}$ . The electronic probability-density distributions of the corresponding atomic procrystals are shown in Figure 10.

Atoms with partially filled valence shells and good overlap possibilities such as the carbon atom will form strong covalent bonds; simultaneously they will exhibit a significant density between the atoms. The density on the bond paths in the atomic procrystal of diamond (Fig. 10a) is  $\geq 1.2 e/\text{\AA}^3$ . In the real crystal, the density on the bond paths is enhanced further to  $\geq 1.9 e/\text{\AA}^3$  owing to covalent bond formation [28].

If the partially filled valence shells are very diffuse (as the  $ns$  AOs of the alkali or alkaline earth atoms) or very compact (as the  $3d$  or  $4f$  AOs of the first transition-metal series or the lanthanides), they cannot overlap well, and density enhancement on the bond path owing to quantum mechanical interference will not occur. If one atom has a loosely bound electron in a diffuse valence orbital and the other atom is strongly electronegative, the atoms will undergo ionic bonding; simultaneously no significant density nor density enhancement is to be expected between the atoms. In Fig. 10b the superimposed CI-densities of Li and F atoms of an atomic [LiF] procrystal are shown, with



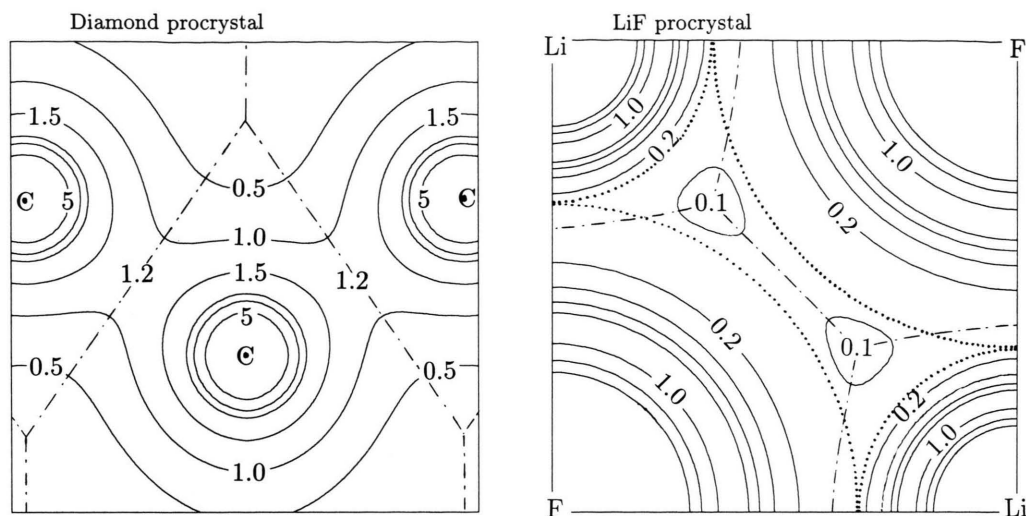
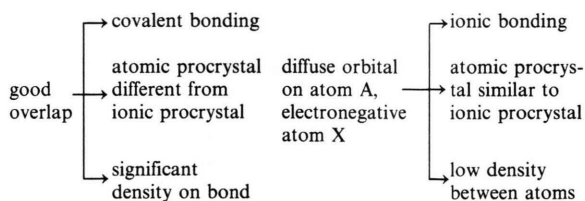


Fig. 10. Electron probability density in a plane through atomic procrytals. a) Diamond [C atom procrytal], contour-line values are 0.5, 1.0, 1.5, 2.0, 3.0, 5.0  $\text{e}/\text{\AA}^3$ ; the lowest density between two bonded atoms is 1.2  $\text{e}/\text{\AA}^3$ . b)  $[\text{Li}^0\text{F}^0]$  (superimposed independent atoms), contour-line values are 0.1, 0.2, 0.3, 0.4, 0.5, 1.0, 1.5, 2.0, 2.5  $\text{e}/\text{\AA}^3$ ; the density between two adjacent atoms drops below 0.2  $\text{e}/\text{\AA}^3$ . The atoms are separated by the minimal-density surface (zero-flux surface of Bader [3]), - · - · -. The dotted circles (· · ·) indicate the standard ionic radii.

the electron density between the atoms as low as 0.1 to 0.2  $\text{e}/\text{\AA}^3$ . Density deformations upon bond formation are similarly small [7, 29], 0.1  $\text{e}/\text{\AA}^3$  on Li–F and 0.2  $\text{e}/\text{\AA}^3$  on Be–F (to be interpreted either as ionic polarization or as atomic covalency). Note the causal relations as represented by the arrows in Diagram 3.

Diagram 3



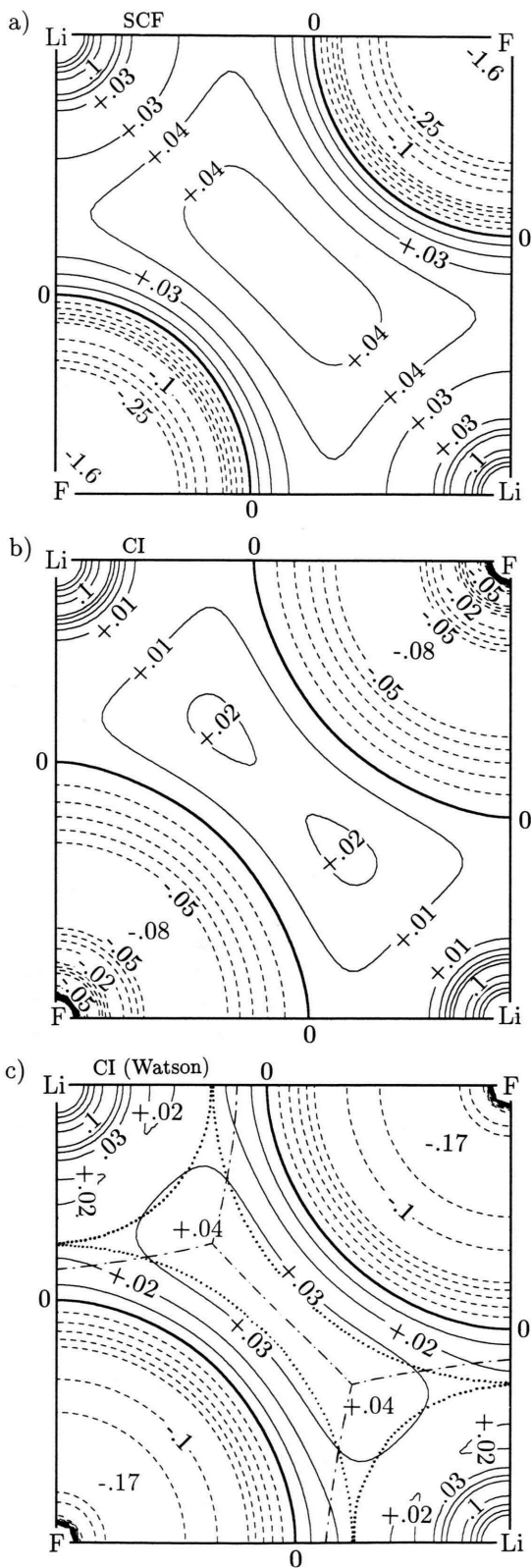
In Fig. 11 we compare atomic and ionic procrytals of  $[\text{LiF}]$ , using the standard Hartree-Fock approximation for the free atoms and ions (Fig. 11 a), correlation-corrected densities (Fig. 11 b), and ionic densities in Watson potentials (Figure 11 c). In the ionic procrytal there is only a very small positive charge density on the  $\text{Li}^+$ , and also in the region between the ions and even in the outer region of the  $\text{F}^-$ -valence shell. A low negative charge density is found near the F nucleus. Accordingly, the excess charge within the minimal-density surface (– · – in Fig. 11 c) with respect to the

overlapping atoms, which can be attributed to the ions, is significantly smaller than  $\pm 1\text{e}$ , namely  $\pm 0.6\text{e}$  at the SCF level and only  $\pm 0.2\text{e}$  at the CI level (it is rather common that electron correlation smoothens charge oscillations). Since the crystal field stabilizes electrons on the negative ions and destabilizes electrons on the positive ions, the effective charges in a procrytal of ions in Watson potentials are again a little larger, namely  $\pm 0.4\text{e}$ . The experimental excess charge densities on F (difference density with respect to the atomic procrytal) in  $\text{Li}_2\text{BeF}_4$  are even smaller ( $\leq 0.06\text{e}/\text{\AA}^3$ ), yielding an excess charge (Hirshfeld charge) of only 0.09 e on F [29].

The so-called spherical electron count function  $N_A(R)$  of atom A at position  $\mathbf{R}_A$  [27],

$$N_A(R) = \int_{r=0}^R 4\pi r^2 dr \cdot \varrho(r_e) \quad \text{with } r = |\mathbf{R}_A - \mathbf{r}_e|, \quad (5)$$

shown in Fig. 12 for Li and F in the  $[\text{LiF}]$  procrytals, demonstrates how similar the charge distributions in atomic and ionic procrytals are, as already mentioned in the introduction (Figure 1). Within the radius of  $R_{\min} = 2.5 a_0$  (corresponding to minimal radial charge density [27]) the electron numbers of fluorine are 9.85 e in  $[\text{Li}^+\text{F}^-]$  and 9.6 e in  $[\text{Li}^0\text{F}^0]$ ; those of lithium at  $R_{\min} = 1.5 a_0$  are 2.03 e in  $[\text{Li}^+\text{F}^-]$  and 2.10 e in  $[\text{Li}^0\text{F}^0]$ .



Our improved atomic and ionic form factors have been used by Seiler [29] to analyse his very accurate X-ray diffraction intensities of  $\text{Li}_2\text{BeF}_4$  (6345 unique reflections up to  $\sin \theta/\lambda = 1.36 \text{ \AA}^{-1}$ ). Using the *approach of comparison* with atomic and ionic procystals, (2) [7, 8], he obtained the following unexpectedly low charges:  $\text{Li}_2^{+0.25}\text{Be}^{+0.50}\text{F}_4^{-0.25}$ . Atomic partial charges obtained with the standard form factors (restricted Hartree-Fock, ions in vacuum [11]) are still smaller:  $\text{Li}_2^{+0.18}\text{Be}^{+0.39}\text{F}_4^{-0.19}$ . Partitioning the total experimental density distribution according to *Hirshfeld's stockholder method* [5] with respect to the present atomic densities yields even lower charges:  $\text{Li}_2^{+0.10}\text{Be}^{+0.16}\text{F}_4^{-0.09}$ . It looks reasonable that half a Be carries the same or slightly less charge than Li or F.

$\text{Li}^{+0.25}\text{F}^{-0.25}$ , as determined by Seiler [29] from experiment using (2), means that the charge distribution on Li and F in the  $\text{Li}_2\text{BeF}_4$  crystal is well approximated by  $1/4 [\text{Li}^+\text{F}^-] + 3/4 [\text{Li}^0\text{F}^0]$  procrytals. The  $[\text{Li}^+\text{F}^-]$  procrytal (correlated ions in Watson potentials) has  $\sim \pm 0.4$  electrons on the ions with respect to  $[\text{Li}^0\text{F}^0]$  (see above) corresponding to charges of  $\pm 0.1$  e for  $1/4 [\text{Li}^+\text{F}^-]$ . LiF cannot be compared directly with  $\text{Li}_2\text{BeF}_4$ : On the one hand, the coordination numbers (CN) in  $\text{Li}_2\text{BeF}_4$  are smaller and Be is less diffuse than Li, both reducing the overlap charge-transfer. On the other hand, the interatomic distances in  $\text{Li}_2\text{BeF}_4$  are comparatively short (corresponding to the lower CN), thus raising the overlap charge-transfer. In any case, the aforementioned  $\pm 0.1$  e are just the excess charge obtained for  $\text{Li}_2\text{BeF}_4$  with Hirshfeld's partitioning approach [29] (see above), where neutral atoms, too, were used as stockholders. However, the observable data may equivalently be interpreted by choosing an ionic  $[\text{Li}^{+1}\text{F}^{-1}]$  procrytal as reference: real  $\text{Li}_2\text{BeF}_4$  with a density contribution of  $3/4 [\text{Li}^0\text{F}^0]$  has charges smaller by  $\frac{3}{4} \cdot (\pm 0.4 \text{ e}) = \pm 0.3 \text{ e}$  on the ions relative to the  $[\text{Li}^+\text{F}^{-1}]$  procrytal, and one might speak of ionic charges of  $\pm 0.7 \text{ e}$ .

Fig. 11. Charge density differences between [LiF] procrytals from atoms and from ions. Contour-line values are 0 (bold line),  $\pm 0.01$ ,  $\pm 0.02$ ,  $\pm 0.03$ ,  $\pm 0.04$ ,  $\pm 0.05$ ,  $\pm 0.1$ ,  $\pm 0.15$ ,  $\pm 0.2$ ,  $\pm 0.25$  e/Å<sup>3</sup>. Negative values (dashed lines) indicate more negative electronic charge density in [Li<sup>+</sup>F<sup>-</sup>] than in [Li<sup>0</sup>F<sup>0</sup>]. a) SCF: Hartree-Fock atoms and ions. b) CI: atomic and ionic densities corrected for electron correlation. c) CI (Watson): dito, but ions in Watson potentials. - - - indicates the minimal-density surface between the atoms, the dotted circles (· · · · ·) indicate the standard ionic radii.

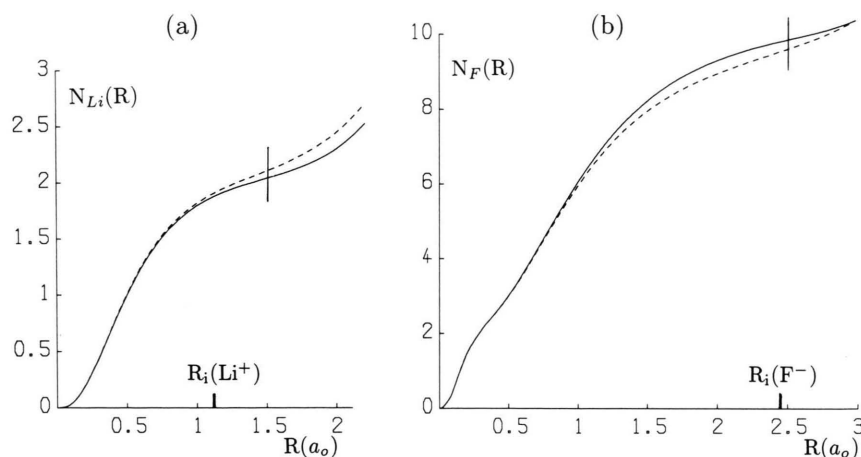


Fig. 12. Electron count functions  $N_A(R)$  around Li (a) and F (b) in [LiF] procystals (number of electrons in a sphere of radius  $R$  (in  $a_0$ ) around the nucleus). — for ionic procystal, --- for atomic procystal. The vertical lines indicate the  $R_{\min}$ -values of the minimal radial charge densities around the respective nuclei. The ionic radii  $R_i$  are also given.

## 7. Discussion, Conclusions and Summary

If the valence shells of atoms in molecules or crystals are non-diffuse (significantly overlapping and forming covalent bonds), homopolar-atomic and heteropolar-ionic charge distributions will be easily distinguishable. Even in this case, partial charges  $q$  on the atoms may be controversial. For CO, for instance,  $q$  is 0.1 to 0.4 according to the approach of Hirshfeld [5], Mulliken [4] or Pauling [30] (where atomic point charges are used to simulate the effects of the charge distribution  $\varrho$ ), whereas Bader [3] gives  $q = 1.35$  (assuming implicitly a multipolar expansion for the atoms).

The situation is even more involved for ionic compounds AX with large CN and the electropositive component A having an extended valence shell. *It is not evident, which partial charges should be assigned to an overlapping atomic procystal  $A^0X^0$  (cf. [29]), since charge overlap of  $A^0$  with  $X^0$  may complementarily be interpreted as charge transfer from  $A^+$  to  $X^-$  (Figure 1). Let us simulate the real charge distribution as*

$$\varrho_{AX} \approx p \varrho_{[A^+X^-]}(v_i) + (1-p) \varrho_{[A^0X^0]}(v_a), \quad (6)$$

where  $p$  is the “ionic” mixing parameter, and  $v_i, v_a$  are parameters monitoring the effective potentials in which the “independent” ions and atoms of the crystal are calculated.

Schwarz et al. [27] have shown that, by setting  $p = 1$  (assumption of integer ionic charges) and  $v_a = 0$  (atoms  $A^0$  and  $X^0$  in vacuum), one can find a  $v_i$  (i.e. modified

Watson radii  $R_w$  for the ions) such that

$$\varrho_{AX} \approx \varrho_{[A^+X^-]}(v_i) \neq \varrho_{[A^0X^0]}(v_a = 0). \quad (7)$$

In general the optimum  $R_w$  that simulates the crystal potential *and* the overlap compression is larger than the  $R_w$  corresponding to the Madelung potential. Seiler and Dunitz [7, 29] have shown that, by setting  $v_a = 0$  and either  $v_i = 0$  (restricted SCF ions in vacuum) or  $v_i = v_M$  (correlated ions in Madelung potential), that is with the *assumption of predefined atoms and ions having charge zero and  $\pm e$ , respectively*, in the two very similar procystals, one can find  $p$ -values so that  $\varrho_{AX}$  is well approximated by (6). We may expect that  $\varrho_{AX}$  can also be approximated by setting  $p = 0$  and adjusting  $v_a$ , the effective potential for atoms in the crystal, to yield

$$\varrho_{AX} \approx \varrho_{A^0X^0}(v_a) \neq \varrho_{[A^+X^-]}(v_i = v_M). \quad (8)$$

It should be stated clearly that the finding of Schwarz (i.e. (7)) is no argument against the fact that one cannot distinguish uniquely between charge overlap and charge transfer. So, we should remember four points.

First, individual atomic charges are not properties uniquely given by nature (and in this respect they cannot be measured), but they are useful and essential concepts that “serve the purpose of summarizing information on electron density distributions in a lapidary though simplifying way” [31] (and in this respect they can be extracted from measurement).

Second, the 3 parameters in (6) are redundant. One may either (a) *assume* that the constituents of the matter

under discussion are ions with integral charges ( $p=1$ ); then the ions must be compressed and polarized appropriately (as, e.g. in [27, 32]). Or one may (b) *assume* that the constituents are atoms ( $p=0$ ); then the atoms must also be deformed appropriately (this can be achieved in the multipole refinement approach [33]). Or one may (c) *predefine* atoms and ions and then determine the charge transfer parameter  $p$  in (6) [7, 8, 29]; then one must explain the physico-chemical meaning of this  $p$ . Defining the atomic charges in  $[\text{Li}^+\text{F}^-]$  to be  $\pm 1$ , and in overlapping  $[\text{Li}^0\text{F}^0]$  to be 0, exaggerates the observable charge transfer from  $[\text{Li}^0\text{F}^0]$  to  $[\text{Li}^+\text{F}^-]$  of about 0.4 e by definition to the integer value of 1 e. Then the experimental charges become  $\pm p$ .

If one does not want to exaggerate the charge transfer, one may define the atomic procrystal  $[\text{A}^0\text{X}^0]$  of an "ionic" compound AX with significantly overlapping, diffuse constituents to have zero atomic charges. With this assumption (b), as, e.g., in [5, 34], one chooses an "atomic" viewpoint, and the atomic charges remain small ( $\pm 0.1$  e for Li, F in the  $\text{Li}_2\text{BeF}_4$  crystal, or  $\pm 0.3$  e to  $\pm 0.6$  e for the LiF molecule [34]). However, in order to accord with the traditional charge scales of chemistry or solid-state physics [4, 30], one must choose assumption (a) that the ionic procrystal  $[\text{A}^+\text{X}^-]$  has integer charges. From this "ionic" viewpoint, Li and F in  $\text{Li}_2\text{BeF}_4$  obtain "experimental" charges of  $\pm 0.7$  e. The formal reason for this situation is that a covalent and an ionic wavefunction are far from being orthogonal, but are rather similar, comparable to the similarity of an MO and a VB function.

Third, in order to determine  $p$  in (6), reliable values of atomic and ionic densities in real and reciprocal

space are needed. They have been calculated here for Li, Be and F. We note that ion formation effects, electron correlation effects, and crystal-field effects on the atomic form factors  $f(k)$  are only important at small  $k/4\pi = \sin \theta/\lambda \leq \frac{1}{3} \text{ \AA}^{-1}$ . Although  $\text{F}^-$  has a rather "soft" charge distribution, correlation and crystal-field effects modify its density  $\varrho(r)$  and form factor  $f(k)$  by not more than a few percent. Although the effects are small, they are not additive (Figure 9). Electron correlation and the crystal field both stabilize  $\text{F}^-$  energetically, but have opposite influences on its form factor and modify the atom-ion difference  $[f(\text{F}^0) - f(\text{F}^-)]$  slightly, mainly in the range of  $\sin \theta/\lambda \in [0.15 \text{ \AA}^{-1}; 0.35 \text{ \AA}^{-1}]$ . So, because of cancellation of errors, simple RHF form factors for  $\text{F}^-$  [11] are still quite useful. Correlation and crystal-field effects on the "hard-core ions"  $\text{Li}^+$  and  $\text{Be}^{+2}$  are negligibly small.

Fourth, the concept of ionic charges becomes more "well-defined" for compact valence orbitals inside the atomic cores ( $d$  and  $f$  elements) and for low coordination numbers.

#### Acknowledgement

We are grateful to W. Weyrich and especially to an unknown referee, and also to B. Engelen, R. Jaquet, H. D. Lutz, P. Seiler, and V. H. Smith, Jr. for many constructive comments; to P. Seiler and V. H. Smith, Jr. for the communication of results prior to publication; and to D. H. Duong for his help in the graphical work. We acknowledge financial support by the Deutsche Forschungsgemeinschaft and by the Fonds der Chemischen Industrie.

- [1] J. Dalton, A New System of Chemical Philosophy, London 1808.
- [2a] J. J. Berzelius, Versuch über die Theorie der chemischen Proportionen und über die chemischen Wirkungen der Electricität, Arnold, Dresden 1820. – M. Faraday, Experimental Researches in Electricity 1832–1838, Reprint, AVG Geest und Portig, Leipzig 1985. – H. von Helmholtz, Faraday Lecture 1881, in: Herrmann von Helmholtz, Vol. 2 (L. Königsberger, ed.), Vieweg, Braunschweig 1903.
- [2b] C. R. A. Catlow and A. M. Stoneham, J. Phys. C **16**, 4321 (1983). – J. Mullay, Structure and Bonding **66**, 1 (1987).
- [3] R. F. W. Bader, Atoms in Molecules, Clarendon, Oxford 1990.
- [4] R. S. Mulliken, J. Chem. Phys. **23**, 1833, 1841 (1955). – R. Heinzmann and R. Ahlrichs, Theoret. Chim. Acta **42**, 33 (1976). – A. E. Reed and F. Weinhold, J. Chem. Phys. **84**, 2418 (1986).
- [5] F. L. Hirshfeld, Theoret. Chim. Acta **44**, 129 (1977).
- [6] R. Daudel, in: The New World of Quantum Chemistry (B. Pullmann and R. Parr, eds.), Reidel, Dordrecht 1976, p. 33.
- [7] P. Seiler and J. D. Dunitz, Helv. Chim. Acta **69**, 1107 (1986).
- [8] W. H. E. Schwarz, K. Ruedenberg, and L. Mensching, J. Amer. Chem. Soc. **111**, 6926, 6933 (1989). – K. Ruedenberg and W. H. E. Schwarz, J. Chem. Phys. **92**, 4956 (1990).
- [9] R. W. James, The Crystalline State, Vol. 2, Bell, London 1948. – J. M. Bijvoet and K. Lonsdale, Phil. Mag. **44**, 204 (1953). – C. R. A. Catlow and A. M. Stoneham, J. Phys. C **16**, 4321 (1983).
- [10] J. C. Slater, Quantum Theory of Molecules and Solids, Vol. 2, McGraw-Hill, New York 1965.
- [11] International Tables for X-Ray Crystallography, Vol. 3 (C. H. MacGillavry and G. D. Rieck, eds.); Vol. 4 (J. A. Ibers and W. C. Hamilton, eds.), Kynoch Press,



- Birmingham 1968, 1974. – J. H. Hubbel, W. J. Veigle, E. A. Briggs, R. T. Brown, D. T. Cromer, and R. J. Howerton, *J. Phys. Chem. Ref. Data* **4**, 471 (1975).
- [12] J. H. Burns and E. K. Gordon, *Acta Cryst.* **20**, 135 (1966).
- [13] J. Almlöf and U. Wahlgren, *Theoret. Chim. Acta* **28**, 161 (1973). – B. Roos and U. Wahlgren, Program Madelung, Theoretical Physics Department, University of Stockholm 1970.
- [14] P. P. Ewald, *Ann. Phys.* **64**, 253 (1921). – F. Bertaut, *J. Phys. Rad.* **13**, 499 (1952).
- [15] R. E. Watson, *Phys. Rev.* **111**, 1108 (1958).
- [16] A. V. Bunge and R. O. Esquivel, *Phys. Rev. A* **33**, 853 (1986). – R. O. Esquivel and A. V. Bunge, *Int. J. Quantum Chem.* **32**, 295 (1987). – R. O. Esquivel, A. V. Bunge, and M. A. Núñez, *Phys. Rev. A* **43**, 3373 (1991).
- [17] R. J. Harrison and N. C. Handy, *Chem. Phys. Lett.* **98**, 97 (1983). – M. R. A. Blomberg and P. E. M. Siegbahn, *Int. J. Quantum Chem.* **14**, 583 (1978). – M. R. A. Blomberg, P. E. M. Siegbahn, and B. O. Roos, *Int. J. Quantum Chem.: Quantum Chem. Symp.* **14**, 299 (1980).
- [18] K. Raghavachari, *J. Chem. Phys.* **83**, 4142 (1985). – S. Huzinaga, *J. Chem. Phys.* **42**, 1293 (1965). – T. H. Dunning, *J. Chem. Phys.* **55**, 716 (1971).
- [19] N. C. Handy, R. J. Harrison, P. J. Knowles, and H. F. Schaefer III, *J. Chem. Phys.* **88**, 4852 (1984). – G. C. Lie and E. Clementi, *J. Chem. Phys.* **60**, 1275 (1974).
- [20] R. J. Buenker and S. D. Peyerimhoff, *Theoret. Chim. Acta* **35**, 33 (1974); **39**, 217 (1975). – R. J. Buenker, S. D. Peyerimhoff, and W. Butscher, *Mol. Phys.* **35**, 771 (1978). – R. J. Buenker, in: *Quantum Chemistry in the 80's* (P. Burton, ed.), University Press, Wollongong 1980; in: *Current Aspects of Quantum Chemistry* (R. Carbo, ed.), Elsevier, Amsterdam 1982.
- [21] F. Sasaki and M. Yoshimine, *Phys. Rev. A* **9**, 17, 26 (1974).
- [22] R. Benesch and V. H. Smith, Jr., *Acta Cryst. A* **26**, 579, 586 (1970).
- [23] P. Kaijser and V. H. Smith, Jr., *Adv. Quantum Chem.* **10**, 44 (1977).
- [24] A. J. Thakkar and V. H. Smith, Jr., *Acta Cryst. A* **48**, 70 (1992). – V. H. Smith, Jr., private communications (1991).
- [25] K. Tanaka and F. Sasaki, *Int. J. Quantum Chem.* **5**, 157 (1971).
- [26] T. Suzuki, *Acta Cryst.* **13**, 279 (1960). – E. Paschalis and A. Weiss, *Theoret. Chim. Acta* **13**, 381 (1969). – P. C. Schmidt and A. Weiss, *Z. Naturforsch.* **34a**, 1471 (1979).
- [27] K. Schwarz, *Phys. Chem. Minerals* **14**, 315 (1987). – J. Redinger and K. Schwarz, *Z. Phys. B* **40**, 269 (1981). – K. Schwarz and H. Schulz, *Acta Cryst. A* **34**, 994 (1978).
- [28] R. Orlando, R. Dovesi, C. Roetti, and V. R. Saunders, *J. Phys. Cond. Matter* **2**, 7769 (1990).
- [29] P. Seiler, in: *Sagamore X Conference on Charge, Spin and Momentum Densities, Collected Abstracts* (M. Springborg, A. Saenz, and W. Weyrich, eds.), Universität Konstanz 1991, p. 118 and *Acta Cryst. B* **49**, in press (1993).
- [30] L. Pauling, *The Nature of the Chemical Bond*, Cornell, Ithaca N.Y. 1960. – J. C. Phillips, *Rev. Mod. Phys.* **42**, 317 (1970). – L. Pauling and J. C. Phillips, *Phys. Today*, Febr. 9 (1971). – W. A. Harrison, *Electronic Structure and the Properties of Solids. The Physics of the Chemical Bond*, Freeman, San Francisco 1980.
- [31] K. Jug and Z. B. Maksić, in: *Theoretical Models of Chemical Bonding*, Vol. 3 (Z. B. Maksić, ed.), Springer, Berlin 1991.
- [32] E. S. Rittner, *J. Chem. Phys.* **19**, 1030 (1951). – L. L. Boyer, M. J. Mehl, J. L. Feldman, J. R. Hardy, J. W. Flocken, and C. Y. Fong, *Phys. Rev. Lett.* **54**, 1940 (1985). – P. W. Fowler and P. Tole, *J. Chem. Soc. Chem. Commun.* **1989**, 1652. – R. Gordon, H. Hummel, and D. Lacks, *Pegasus*, Harvard, Cambridge MA 1990.
- [33] P. Coppens, in: *Electron Distributions and the Chemical Bond* (P. Coppens and M. B. Hall, eds.), Plenum, New York 1982.
- [34] E. N. Maslen and M. A. Spackman, *Aust. J. Phys.* **38**, 273 (1985).